On the Use of Shape-Constrained Splines for Biokinetic Process Modeling ⋆

Alma Mašić * **Sriniketh Srinivasan** ** **Julien Billeter** **
Dominique Bonvin ** **Kris Villez** *

* *Eawag: Swiss Federal Institute of Aquatic Science and Technology, Überlandstrasse 133, P.O. Box 611, CH-8600 Dübendorf, Switzerland*
** *Laboratoire d'Automatique, Ecole Polytechnique Fédérale de Lausanne, CH-1015 Lausanne, Switzerland*
(e-mail: kris.villez@eawag.ch)

Abstract: Identification of mathematical models is an important task for the design and the optimization of biokinetic processes. Monod or Tessier growth-rate models are often chosen by default, although these models are not able to represent the dynamics of all bacterial growth processes. This imperfect representation then affects the quality of the model prediction. This paper introduces an alternative approach, which is based on constraints such as monotonicity and concavity and the use of shape-constrained spline functions, to describe the substrate affinity with high parametric flexibility. This way, the difficult task of searching through potentially incomplete rate-model libraries can be circumvented. A simulated case study is used to illustrate the superiority of the proposed method to represent non-ideal growth conditions, where neither Monod nor Tessier kinetics offer a good approximation.

Keywords: mathematical models; microbial growth-rate kinetics; Monod equation; shape-constrained spline function; wastewater treatment

1. INTRODUCTION

The characterization of the growth of a bacterial population has been important since the early days of the field of microbiology, (Scott and Hwa, 2011). The growth processes of many different bacterial species have been described in countless works, with the most prominent ones being Monod (1949) and Tessier (1942). The proposed models establish a correlation between the biomass growth rate and the concentration of the limiting nutrient (Monod, 1949). Conventional biological wastewater treatment processes make use of bacterial growth and decay as a means to remove unwanted compounds such as organic matter, nitrogen, and phosphorus. Decentralized wastewater treatment, in contrast to a centralized system, is spread out over many different locations at which relatively smaller reactors are operated. In situations where monitoring and reactor operation relies on the use of soft sensors (Mašić and Villez, 2014), it is crucial to identify reliable process models for different decentralized reactors and to facilitate model updates over time. Mathematical models of wastewater treatment processes have long been used to describe these processes (Wanner et al., 2006; Henze et al., 2008). To obtain reliable predictions, it is often necessary to identify *dynamic* models on the basis of dedicated experiments. The Monod growth-rate model is often chosen by default in biological wastewater treatment modeling. However, when the Monod model does not capture the behavior of certain groups of bacteria, this model is not suitable for use in process design and optimization (Neumann and Gujer, 2008).

In almost every bacterial growth process, one can describe substrate affinity as a monotonically increasing (isotonic) rate law with a concave shape. This qualitative feature is used in the construction of shape-constrained spline (SCS) functions which are constrained to be of isotonic and concave shape yet flexible enough to approximate any effect of the substrate corresponding to such a shape. As such, the chosen SCS function serves as a near-universal biokinetic growth model and can approximate any isotonic and concave rate laws that may be found in a conventional and necessarily incomplete library of candidate growth-rate models (Refsgaard et al., 2006).

Shape restrictions are commonly applied for fitting hazard models (Meyer, 2008). More recently, SCS functions were adopted for fault detection and fault diagnosis in a qualitative trend analysis framework (Villez et al., 2013; Villez and Habermacher, Submitted). Formal approaches to use qualitatively described information have also been proposed to facilitate automated selection of candidate models. In Schaich and King (1999) and Schaich et al. (2001), such information is obtained by means of qualitative simulation (QSIM), and in Madár et al. (2003), this information is considered available as prior knowledge. In contrast to previous studies, this study is focused on identifying the most likely shape of the kinetic rate laws governing the modeled process – not the shape of the obtained measurement trends. This is achieved by placing the proposed shape constrained spline function as a rate law inside a model described by an ordinary differential

⋆ This study is financed by Eawag Discretionary Funds (PSP: 5221.00492.009.03).

equation (ODE). This particular use of SCS functions for dynamic modeling is proposed for the first time in this contribution. Thanks to the enforced shape restrictions, the resulting models can be interpreted in the same way as any conventional white-box model, while exhibiting the parametric flexibility and generality of typical black-box models.

The paper is organized as follows. Section 2 presents the common growth-rate models, the concept of shape-constrained spline functions and its numerical implementation. Section 3 illustrates the advantages and drawbacks of fitting the kinetic models to either measured rates or measured concentrations by means of a simulated example. Finally, Section 4 concludes the paper.

2. MATHEMATICAL MODEL & METHODS

2.1 Model description

This paper focuses on a very simple model describing bacterial growth through consumption of a substrate. The model construction can be interpreted as a simplification of the activated sludge models discussed in Henze et al. (2008). Let $S := c_S(t)$ denote the substrate concentration at time t. The change in substrate concentration with respect to time can be expressed as

$$\frac{dS}{dt} = -r(S), \quad S(0) = S^0 \tag{1}$$

where $r(S) := r\big(c_S(t)\big)$ is a rate law expressing the bacterial growth and $S^0 := c_S(0)$ denotes the initial substrate concentration. The product concentration, denoted as $P := c_P(t)$, can be computed as

$$P = S^0 - S. \tag{2}$$

The growth-rate expression $r(S)$ can be defined in different ways based on the biological phenomena, substrates and products that are involved. In this study, a family of rate models based on uninhibited bacterial growth is considered. When the growth rate for a specific biological reactor is not known, one has to test several rate laws among this model family. Two rate laws of this family are described in the next section.

2.2 Library of growth-rate models

The default bacterial growth-rate model used in wastewater treatment modeling is the Monod growth rate,

$$r_M(S) = a^{max}\frac{S}{K_S + S} \tag{3}$$

where a^{max} denotes the maximum activity of the biomass and K_S is the affinity constant. For the purposes of this paper, a^{max} is a lumped parameter incorporating the maximum specific growth rate, the total biomass, and the yield coefficient, all of which are assumed constant during the experiment, that is, the net growth is assumed to be zero.

Another rate law that is used to describe bacterial growth is the Tessier growth rate,

$$r_T(S) = a^{max}\left(1 - e^{-S/K_S}\right). \tag{4}$$

Both the Monod and Tessier models are monotonically increasing, with a steep increase for small values of S and a saturated response at high values of S. Each model has two parameters that need to be determined, namely a^{max} and K_S. However, regardless of their similarity, there exists no parametrization of these rate laws that ensures that their values are the same for every substrate concentration: the two rate laws intersect at $S = 0$ and at at most in two more points for $S > 0$.

2.3 Shape-constrained spline functions

As an alternative to the above library of rate models, a single shape-constrained spline function is used to approximate all growth-rate models. The use of the SCS function is justified by the fact that it shares the concave and monotonically increasing (isotonic) behavior and a zero offset (i.e., it passes through the origin) with the rate laws in the library.

In this study, a cubic B-spline basis (see Ramsay and Silverman (2002)) is used. This rate law is a piecewise cubic polynomial in the substrate concentration and is, as will be shown below, a convenient functional basis to use with shape constraints. One can write the growth-rate model as a weighted sum of spline basis functions as

$$r_{SCS}(S) = \mathbf{b}_0\,(S)^{\mathrm{T}}\,\boldsymbol{\theta} \tag{5}$$

with $\mathbf{b}_0(S)$ the (n_k+3)-dimensional vector of spline basis functions evaluated at the substrate concentration S, and $\boldsymbol{\theta}$ the (n_k+3)-dimensional vector of model parameters, as in previous works (Villez et al., 2013; Villez and Habermacher, Submitted). The piecewise behavior is controlled by the location of the n_k+1 knots (or n_k segments) placed equidistantly between S_0 and S_{n_k}. For the simplicity of notation, the location of these knots are further referred to as $\{S_0, S_1, \ldots, S_{n_k}\}$ with n_k being the number of piecewise polynomial segments.

For polynomial functions of any order and on a nonempty domain, shape constraints can be specified as a finite number of semi-definite cone constraints (Nesterov, 2000). In special cases, these inequality constraints can be reduced to second-order cone constraints. This property has been exploited by Papp and Alizadeh (2014), Villez et al. (2013), and Villez and Habermacher (Submitted) to fit, in the maximum-likelihood sense, spline functions to univariate data series. However, in the present example (concave isotonic shape with zero offset), the following linear constraints are sufficient to ensure the desired shape:

$$\mathbf{b}_0(S^0)^{\mathrm{T}}\boldsymbol{\theta} = 0 \tag{6}$$

$$\mathbf{b}_1(S_k)^{\mathrm{T}}\boldsymbol{\theta} \geq 0 \tag{7}$$

$$\mathbf{b}_2(S_k)^{\mathrm{T}}\boldsymbol{\theta} \leq 0 \quad \forall k = 0, 1, \ldots, n_k \tag{8}$$

with $\mathbf{b}_1(\cdot)$ and $\mathbf{b}_2(\cdot)$ the first and second derivatives of the cubic spline basis functions.

In previous work by Villez et al. (2013) and Villez and Habermacher (Submitted), the shape-constrained spline functions were fitted directly to data pairs consisting of values for the function input (substrate concentration) and output (growth rate). By maintaining the function fitting problem in this format and assuming Gaussian noise in the growth-rate measurements, the maximum likelihood estimation problem becomes a quadratic problem subject to linear constraints. This convex problem can easily

be solved to global optimality, even if the number of parameters is large.

Unfortunately, one cannot obtain direct measurements of the growth rates in practice. Instead, one relies on dynamic experiments during which concentrations of the substrate(s) and product(s) are measured. To fit a rate model to such data, it is necessary to differentiate the measured time series, which leads to noise amplification, or else to integrate the rate model and predict the concentrations. The latter option is chosen here. However, this choice implies that the fitting problem becomes nonlinear in the parameters of the spline function.

2.4 Model fitting

Experiments are performed by simulating bacterial growth rate laws and generating appropriate measurements. These measurements are used to fit the rate models from the library and the proposed SCS model. All computations are performed with Matlab (The Mathworks, 2015) and the Functional Data Analysis toolbox by Ramsay and Silverman (2002). The parameters used in all simulated case studies are shown in Table 1.

Table 1. Parameter values used in the simulation experiments.

Parameter	Value	Unit
S_0	25	mg N/L
a^{max}	11	mg N/L·d
K_S	2	mg N/L
σ	0.5	mg N/L

The first study consists of fitting rate models to noise-free rate measurements that have been generated using a specific rate model evaluated at $N = 2501$ points (substrate concentrations) Noise-free measurements are used in this case to demonstrate approximation properties. The parameters of the Monod and Tessier models are determined by regression using the Matlab built-in nonlinear least-squares optimizer `lsqnonlin`. The parameters of the SCS model are obtained through solving this as a second-order cone program (SOCP) with an interior-point algorithm. The number of parameters is chosen by the user by selecting the number of knots between S_0 and S_{n_k} at which the spline function is evaluated. To cover the entire range of substrate concentrations, the first and final knots are set to $S_0 = 0$ mg N/L and $S_{n_k} = 26$ mg N/L. Two cases are considered: In the first case denoted *SCS1*, an increment of 5.2 mg N/L is used, resulting in a spline model with 8 parameters; in the second case denoted SCS2, an increment of 1 mg N/L is used, leading to 29 parameters for the spline model.

The second study consists of fitting the rate models by comparing the measured concentrations with the predicted concentrations obtained via integration of the differential equation (1). The concentrations used were the substrate concentration S and the product concentration P. The simulated measurements are obtained by solving equations (1)-(2) with a specific rate model $r(S)$ for $t = [0, 4]$ h, sampling the time series every 2.5 min, which yields $N = 97$ time points, and adding zero-mean Gaussian noise of standard deviation $\sigma = 0.5$ to each measurement. The regression procedure is as follows:

(1) In Step 1, the concentration measurements of the substrate over time are differentiated to obtain the measured growth rates;
(2) In Step 2, the rate models from the library and the SCS model are fitted to these rate measurements by adjusting their respective parameters, resulting in initial guesses $(a^{max})_0$, $(K_s)_0$ and $(\boldsymbol{\theta})_0$ for the next step;
(3) In Step 3, the measured and modeled concentrations are compared for each rate candidate by solving Eqs. (1)-(2) with `ode15s` and adjusting their respective parameters, resulting in parameter values $\hat{a}^{max}$, $\hat{K_s}$ and $\hat{\boldsymbol{\theta}}$.

This procedure is summarized in Table 2. Steps 1 and 2 are required to obtain initial guesses for the parameter optimization in Step 3.

Table 2. Numerical procedure for fitting rate models to concentrations.

Step	Library models	SCS model	Result
1.	$\dot{\hat{S}}$	$\dot{\hat{S}}$	$\hat{r}$
2.	fit of $\hat{r}$ with `lsqnonlin`	fit of $\hat{r}$ with `fmincon`	$(a^{max})_0$, $(K_s)_0$ and $(\boldsymbol{\theta})_0$
3.	fit of $\tilde{S}$ with `fminunc`	fit of $\tilde{S}$ with `fmincon`	$\hat{a}^{max}$, $\hat{K_s}$ and $\hat{\boldsymbol{\theta}}$

3. RESULTS & DISCUSSION

In Section 3.1, we present and discuss the results obtained with simulated noise-free rate measurements. Section 3.2 covers the results obtained with simulated noisy substrate and product concentration measurements.

3.1 Fitting rate parameters to measured rates

In a first scenario, the measured growth rate is simulated as a Monod model. Simulated data are used to fit both the growth-rate models from the library and the SCS models. Figure 1 shows the 8 cubic B-spline basis functions of order 4.

The Monod and Tessier models are fitted to measured growth-rate data using the fitting approach described in Section 2.4. Also, two SCS models are fitted to the data. Figure 2 shows the *in silico* measured (Monod) rate, the fitted Monod rate and the two fitted SCS rates. It is easy to see that all models fit the data very well since the curves are almost indistinguishable. A similar figure is obtained when the Tessier model is used to simulate the rate measurements, and the Tessier and two SCS models are then fitted to the data (not shown). In these cases, an SCS model is able to approximate a known measured growth-rate model such as the Monod or Tessier model.

In a second scenario, we assume that the true growth rate is unknown a priori and is not part of the library described in Section 2.2. However, the unknown rate law is assumed to exhibit a similar shape as before. We now consider three such unconventional rate laws, namely, the hyperbolic tangent law r_{ht}, a Monod+Tessier law r_{MT}, and the root law r_r:

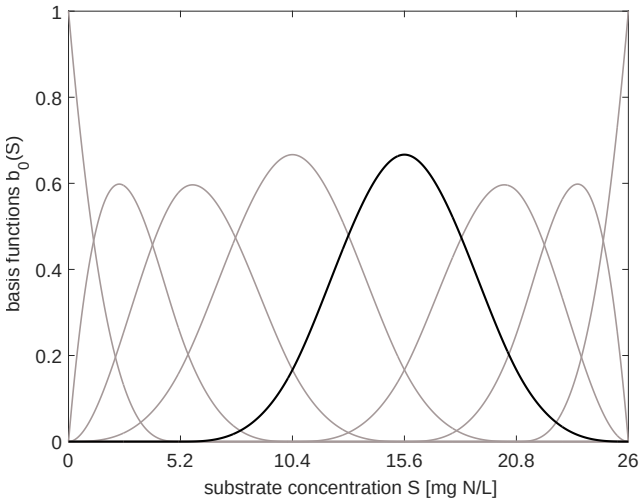

Fig. 1. Cubic B-spline basis functions using 6 knots. The knots are indicated on the x-axis. All basis functions are defined on the entire domain, but they are constrained to be non-zero in a limited segment of the domain. The black curve illustrates a single basis function. The other basis functions are translated and dilated versions of the black curve, except at the domain boundaries. The functions are determined by the knot locations.

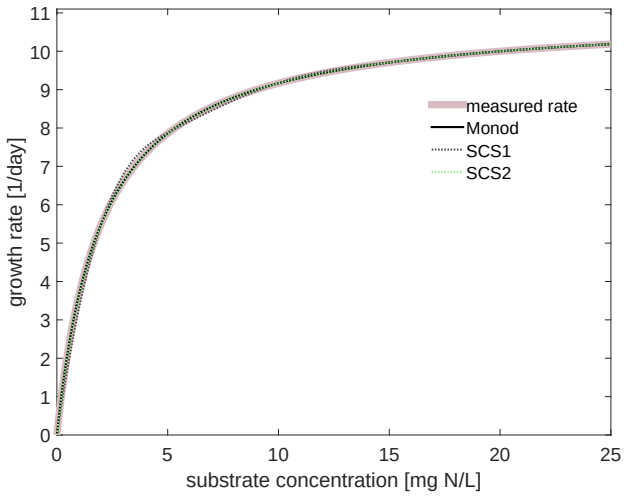

Fig. 2. Monod growth rate [1/day] as a function of the substrate concentration [mg N/L]: noise-free measured rate, Monod model, *SCS1* model (6 knots), *SCS2* model (27 knots).

$$r_{ht}(S) = a^{max} \tanh\left(\frac{S}{K_S}\right) \tag{9}$$

$$r_{MT}(S) = \frac{a^{max}}{2}\left(\left(1 - e^{-\frac{S}{K_S}}\right) + \frac{S}{K_S + S}\right) \tag{10}$$

$$r_r(S) = a^{max}\frac{\sqrt{\frac{5S}{\sqrt{1.5}} + 4} - 2}{\sqrt{\frac{5S}{\sqrt{1.5}} + 4} - 2 + K_S} \tag{11}$$

where $a^{max} = 11$ and $K_S = 2$ in all rate laws. Each rate law is used to simulate the measured rates to which the Monod and Tessier models and two SCS models will be fitted. For these unconventional rate laws, which exhibit the same qualitative behavior but are not present in the library, the SCS model is expected to fit the data well, while the fits of the Monod and Tessier models should be worse.

Quality of fit is measured by computing the root mean square residual

$$\mathrm{RMSR}_{j,k} = \sqrt{\frac{1}{N}\sum_{i=1}^{N}\left(r_j(S_i) - r_k(\hat{S}_i)\right)^2} \tag{12}$$

where $j \in \{M, T, ht, MT, r\}$ is the simulated growth rate, $k \in \{M, T, SCS1, SCS2\}$ is the candidate growth-rate model, S is the noise-free substrate concentration, and $\hat{S}_{k,i}$ is the modeled substrate concentration obtained with the candidate rate k, at time point t_i, with $i = 1, \ldots, N = 2501$ measurements. The RMSR values are shown in Figure 3. The horizontal axis lists the five simulated rate laws. The RMSR values indicate some differences in performance between the four candidate models:

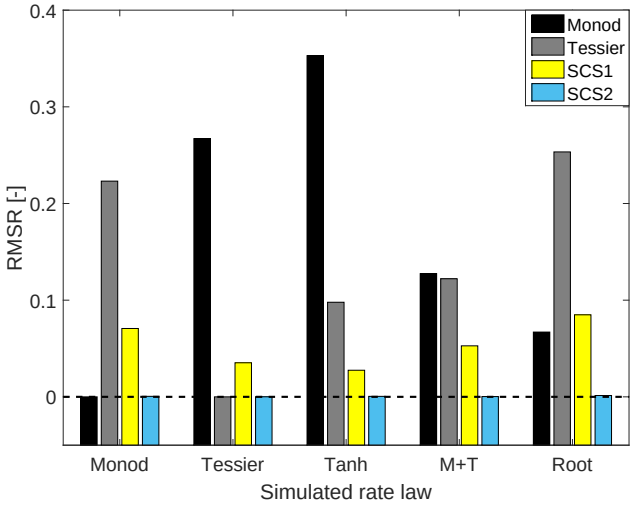

Fig. 3. RMSR values upon fitting the Monod, Tessier, and two SCS models to growth-rate measurements corresponding to five simulated rate laws (Monod, Tessier, hyperbolic tangent, Monod+Tessier, square root).

(1) For the measured Monod rate law, the Tessier model has the worst fit, which comes as no surprise since the two laws cannot be adjusted to overlap. As expected, the Monod model has a perfect fit, while the SCS model improves with the number of knots.
(2) An analogous behavior is observed when the Tessier rate is measured: the Tessier model fits perfectly, while the Monod model is poor and the quality of the SCS model increases with the number of knots.
(3) The ability of the conventional rate law candidates to approximate the unconventional rate laws can vary significantly. For example, the simulated root law is better fitted by the Monod than the Tessier model. The simulated hyperbolic tangent rate law cannot be fitted with the Monod or Tessier models. For the simulated Monod+Tessier rate laws, the Monod and Tessier models provide a relatively equal fit.

(4) Both SCS models deliver a better fit than the Monod and Tessier models when hyperbolic tangent and Monod+Tessier rate laws are used for simulation. The *SCS2* model leads to a universally good fit for all simulated rate laws. This demonstrates a near-universal approximation property of the SCS functions, i.e., an isotonic-concave SCS will approximate any rate law with the same shape to any level of precision as the spline knot resolution is increased.

3.2 Fitting rate parameters to measured concentrations

Since it is rather uncommon to measure growth rates directly, a different case is studied in this section. The growth-rate model is now part of the ordinary differential equation (1) describing the substrate concentration over time in a biological reactor. The Monod growth rate is used to simulate the concentrations in Figure 4. In the biological reactor, bacteria convert the substrate S to a product P. We see that the concentration of the substrate decreases with time until it is completely depleted. The simulated data points are corrupted with additive noise ($\sigma = 0.5$). The product displays an opposite behavior compared to that of the substrate, starting from 0 mg N/L and increasing with time until all substrate has been converted.

Figure 4 shows the fit of the Monod and SCS models to both S and P concentrations. Both models approximate the measured data very well. The SCS model used in this scenario is *SCS1* with 6 knots.

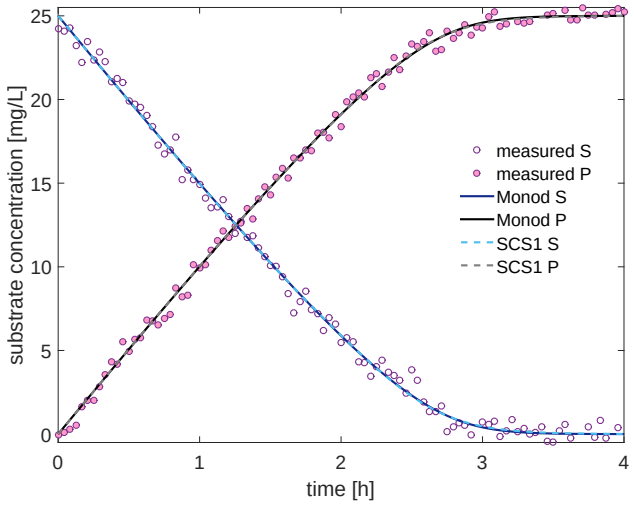

Fig. 4. Substrate S and product P concentration measurements in a biological reactor simulated with Monod growth rate. Fitting of the Monod and *SCS1* models to the measured concentrations, one model at a time.

Computation of the weighted root mean square residuals (WRMSR) provides a more detailed comparison of the fit quality. The WRMSR values are obtained by computing the RMSR values as in (12) and dividing by the standard deviation σ:

$$\mathrm{WRMSR}_{j,k} = \frac{1}{\sigma}\left(\sqrt{\frac{1}{N}\sum_{i=1}^{N}\left(\tilde{S}_j(t_i) - \hat{S}_k(t_i)\right)^2}\right) \qquad (13)$$

where $j \in \{M, T, ht, MT, r\}$ is the measured growth rate, $k \in \{M, T, SCS1, SCS2\}$ is the candidate growth-rate model, $\tilde{S}_{j,i}$ is the noisy measured substrate concentration (obtained with the true rate j), and $\hat{S}_{k,i}$ is the modeled substrate concentration obtained with the candidate rate k, at time point t_i, with $i = 1, \ldots, N = 97$.

The WRMSR values for the case in Figure 4 are very close between the Monod and the SCS model. Both models fit the S and P concentrations well. Figure 5 shows the S and P residuals. These residuals, which are computed with respect to the noisy simulated values, are plotted with indication of the $2\,\sigma$ measurement error band. We see that most residuals are within the $2\,\sigma$ band.

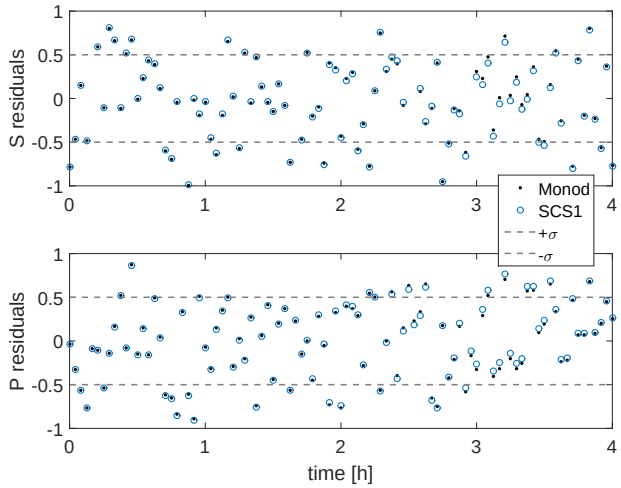

Fig. 5. Substrate and product residuals between the noisy simulated and the modeled concentrations using both the Monod and SCS models, with the $2\,\sigma$ measurement error band. Note that the simulated concentrations were generated using the Monod rate law.

The same exercise is repeated for all five growth rate laws as measured rates, namely, Monod, Tessier, root, hyperbolic tangent, and Monod+Tessier. In each case, the parameters of the Monod, Tessier and SCS models are fitted. The WRMSR values are computed to facilitate further comparison. Here, the residuals for S and P are computed together (with $N = 2 \cdot 97$ in equation (13)) to obtain a single WRMSR value, taking into account the fit for both substrate and product. Figure 6 shows a summary of the performance of the different growth-rate models. The behavior is similar to that observed in Figure 3, with the Monod model having the best fit for the measured Monod rate law, and the Tessier model having the best fit for the measured Tessier rate law. When the other growth-rate laws are simulated, the performance of the Monod and Tessier models varies. In contrast, the optimized SCS model has an excellent fit in all cases, even with as few knots as 6 that were used in this case. This suggests that the SCS model with the selected isotonic-concave shape is likely to fit well to data produced with any known or unknown growth rate law exhibiting the same shape.

Note that the use of the SCS approach can be advantageous in a decentralized system, where the model identification needs to be performed for each reactor. As long as the assumed shape remains valid, the SCS model will

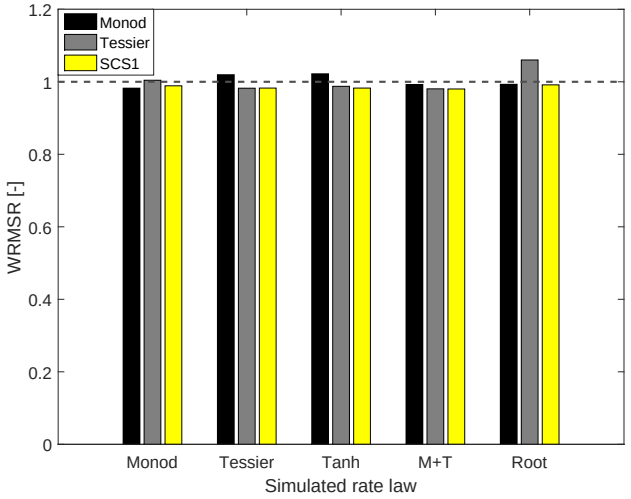

Fig. 6. WRMSR values for the Monod, Tessier and SCS models fitted to concentrations generated by five simulated growth-rate laws (Monod, Tessier, hyperbolic tangent, Monod+Tessier, square root).

achieve a good fit. Conversely, if the optimization results in a bad fit, this could be interpreted as an indication that the *shape* of the growth-rate law has changed, that is, the behavior of the bacteria differs from that assumed by the modeler. This approach could serve as a diagnostic tool in the model identification process. This, however, assumes that the parameter estimation problem can be executed to acceptable optimality. Current results suggest that this is indeed possible (Mašić et al., 2016).

4. CONCLUSIONS

The SCS model can fit all investigated growth-rate laws and requires less computational efforts than searching through a library of rate laws. When faced with an unconventional growth rate that is not already part of the library, the SCS approach allows identification of well-fitting model as long as the assumed shape is valid. Furthermore, the proposed SCS models deliver a consistently good fit for all the five simulated rate laws, thus exhibiting a near-universal approximation property. This is not possible with conventional Monod and Tessier growth-rate models. Finally, the SCS models are interpreted in the same white-box way as any conventional rate law, despite its black-box nature.

Future work aims at using the SCS approach for diagnosis, that is, for determining whether an observed growth rate belongs to a set of known growth rate laws. At the same time, the fitting of SCS models with more complex shapes, e.g. expressing substrate inhibition, is under investigation.

REFERENCES

Henze, M., van Loosdrecht, M., Ekama, G., and Brdjanovic, D. (eds.) (2008). *Biological wastewater treatment: Principles, modelling and design*. IWA Publishing.

Madár, J., Abonyi, J., Roubos, H., and Szeifert, F. (2003). Incorporating prior knowledge in a cubic spline approximation – application to the identification of reaction kinetic models. *Ind. Eng. Chem. Res.*, 42, 4043 – 4049.

Mašić, A., Udert, K.M., and Villez, K. (2016). Global parameter optimization for biokinetic modeling. *Environmental Modelling & Software*. Submitted.

Mašić, A. and Villez, K. (2014). Model-based observers for monitoring of biological nitrification of urine in decentralized treatment. *Proceedings of the 2nd IWA Specialist Conference on EcoTechnologies for Sewage Treatment Plants*, Verona, Italy(23–27 June).

Meyer, M.C. (2008). Inference using shape-restricted regression splines. *Annals of Applied Statistics*, 2, 1013–1033.

Monod, J. (1949). The growth of bacterial cultures. *Ann. Rev. Microbiol.*, 3, 371–394.

Nesterov, Y. (2000). *High Performance Optimization, Applied Optimization*, volume 33, chapter Squared functional systems and optimization problems, 405–440. Kluwer Academic Publishers.

Neumann, M. and Gujer, W. (2008). Underestimation of uncertainty in statistical regression of environmental models: influence of model structure uncertainty. *Environ. Sci. Technol.*, 42(11), 4037–4043.

Papp, D. and Alizadeh, F. (2014). Shape-constrained estimation using nonnegative splines. *Journal of Computational and Graphical Statistics*, 23, 211–231.

Ramsay, J. and Silverman, B. (2002). *Applied functional data analysis: Methods and case studies*. Springer-Verlag, New York.

Refsgaard, J., der Sluijs, J.V., Brown, J., and der Keur, P.V. (2006). A framework for dealing with uncertainty due to model structure error. *Adv. Water Resour.*, 29(11), 1586–1597.

Schaich, D., Becker, R., and King, R. (2001). Qualitative modelling for automatic identification of mathematical models of chemical reaction systems. *Control Engineering Practice*, 9.

Schaich, D. and King, R. (1999). Qualitative modelling and simulation of chemical reaction systems. *Computers and Chemical Engineering Supplement*, S415–S418.

Scott, M. and Hwa, T. (2011). Bacterial growth laws and their applications. *Curr. Opin. Biotechnol.*, 22(4), 559–565.

Tessier, G. (1942). Croissance des populations bactériennes et quantité d'aliment disponible. In *Review Science extrait du No. 3208*, 209–214.

The Mathworks (2015). MATLAB online documentation. URL `http://www.mathworks.com/help/matlab/`. Accessed on October 28, 2015.

Villez, K. and Habermacher, J. (Submitted). Shape anomaly detection for process monitoring of a sequencing batch reactor. *Comp. Chem. Eng.*

Villez, K., Venkatasubramanian, V., and Rengaswamy, R. (2013). Generalized shape constrained spline fitting for qualitative analysis of trends. *Comp. Chem. Eng.*, 58, 116–134.

Wanner, O., Eberl, H., Morgenroth, E., Noguera, D.R., Picioreanu, C., Rittmann, B., and van Loosdrecht, M. (2006). Mathematical modeling of biofilms. In *Scientific and Technical Report No.18*. IWA Publishing.